Experimental chronic jet lag promotes growth and lung metastasis of Lewis lung carcinoma in C57BL/6 mice

MINGWEI WU[1,2,6], JING ZENG[1,3], YANFENG CHEN[1,4], ZHAOLEI ZENG[1,2], JINXIN ZHANG[1,5], YUCHEN CAI[1,2], YANLI YE[1,2], LIWU FU[1,2], LIJIAN XIAN[1,2] and ZHONGPING CHEN[1,6]

[1]State Key Laboratory of Oncology in South China; Departments of [2]Research, [3]Pathology, and [4]Head and Neck Cancer, Cancer Center, Sun Yat-Sen University; [5]Department of Medical Statistics and Epidemiology, Sun Yat-Sen University; [6]Department of Neurosurgery, Cancer Center, Sun Yat-Sen University, Guangzhou, Guangdong, P.R. China

Received December 8, 2011; Accepted January 17, 2012

DOI: 10.3892/or.2012.1688

Abstract. Circadian rhythm has been linked to cancer genesis and development, but the detailed mechanism by which circadian disruption accelerates tumor growth remains unclear. The purpose of this study was to investigate the effect of circadian disruption on tumor growth and metastasis in male C57BL/6 mice, using an experimental chronic jet lag model. Lewis lung carcinoma cells were inoculated into both flanks of the mice following 10 days of exposure to experimental chronic jet lag or control conditions. The effects on tumor growth and lung metastasis were assessed, and the effect on gene expression was detected using cDNA microarrays and real-time quantitative RT-PCR. Tumors grew faster in the experimental chronic jet lag mice compared to the control mice (P=0.004). Lung metastases were found in 10 out of 24 mice in the chronic jet lag group, but only in 3 out of 24 mice in the LD group (P=0.023). Microarray data showed that in both liver and tumors circadian disruption altered the expression of genes, including those related to the cell cycle, apoptosis, the immune response and metastasis suppressor genes. The expression of the NDRG1 gene was suppressed by chronic jet lag. We conclude that circadian disruption can promote tumor progression and metastasis by affecting the expression of both tumor-related genes and metastasis suppressor genes.

Introduction

Most living organisms, from cyanobacteria to plants, insects, and mammals, are capable of displaying spontaneously sustained oscillations with a period close to 24 h, known as 'circadian rhythm'. Studies have found that circadian rhythms are governed by a biological clock. The mammalian circadian clock contains three components: input pathways, a central pacemaker and output pathways. The mammalian central pacemaker is located in the suprachiasmatic nuclei (SCN) of the anterior hypothalamus and controls the activity of the peripheral clocks through the neuroendocrine and autonomic nervous systems (1,2). Circadian rhythms govern the rhythmic changes in the behavior and/or physiology of mammals, such as body temperature, blood pressure, hormone production, digestive secretion, neurotransmitter secretion, and even gene expression (1,3-6).

Circadian rhythms have been found to play a very important role in cancer genesis and development. Fu *et al* showed that mutant mice deficient in the period homolog 2 (*Per2*) gene, a core circadian-clock gene, had a more marked increase in tumor development after gamma radiation than the wild-type mice (7,8). Wood *et al* showed that mutation of the *Per2* gene accelerated ApcMin/$^{+}$ tumorigenesis in mice (11). Malignant growth was accelerated by the disruption of circadian coordination that resulted from SCN destruction or experimental chronic jet lag (8-11). In contrast, overexpression of *Per1*, another core circadian gene, in human cancer cell lines can lead to significant growth reduction (12). Although circadian rhythms have been linked to cancer, the detailed mechanism by which circadian disruption accelerates tumor growth remains unclear.

Therefore, we hypothesized that circadian disruption might disrupt the expression of the clock genes and other tumor-related genes that could lead to a decrease in the level of the antitumor response. This study on Lewis lung carcinoma (LLC) cells investigated the effects of experimental chronic jet lag on growth, lung metastasis, and gene expression, which was detected using the global genomic gene scan.

Materials and methods

Ethics statement. All research involving animal experiments was approved by the Animal Ethics Committee of the Cancer Center, Sun Yat-sen University (approved ID, NSFC30500589).

Animals and synchronization. A total of 48 male, 4-week-old C57BL/6 mice (Vital River Laboratory Animal Technology

Correspondence to: Dr Mingwei Wu or Zhongping Chen, State Key Laboratory of Oncology in South China, Cancer Center, Sun Yat-Sen University, Guangzhou, Guangdong 510060, P.R. China
E-mail: wumw@mail.sysu.edu.cn
E-mail: chenzhp@sysucc.org.cn

Key words: jet lag, circadian rhythm, tumor, metastasis, mouse

Co., Ltd., Beijing, China) were housed and kept in an autonomous chronobiological facility (Suzhou Anke Purification Equipment Factory, China) equipped with temperature control (23±1˚C). Mice were kept in six compartments, each provided with filtrated air (700 m^3/h), but with the potential to apply separate lighting regimens (300 Lux). Four mice were housed per cage. The mice were synchronized to a daily light: darkness ratio of 12 h light and 12 h darkness (LD 12:12) for 2 weeks. Food (normal chow, Medical Laboratory Animal Centre of Guangdong, China) and water were supplied *ad libitum*. The mice were subsequently randomized into two groups: half (n=24) became the experimental chronic jet lag (CJL) group, who were exposed to the jet lag light scheme created by advancing the light onset by 8 h every 48 h; the remainder (n=24) served as the unshifted control group (LD), who stayed in the LD 12:12 conditions (Fig. 1) (6).

Body temperature. Rectal temperature was measured twice during the experiment (after 2 weeks of synchronization and after 10 days of jet lag) using a digital thermometer (Omron™-MC612, Omron Dalian Co., Ltd., China). Rectal temperatures of all of the mice in the LD group were measured at six zeitgeber time (ZT) points (ZT3, 7, 11, 15, 19, and 23) within 48 h (where ZT12 was lights off). In the CJL group, the rectal temperatures of the mice were measured at the same local time (Beijing time) and corresponding time points were labeled as ZT3x, 7x, 11x, 15x, 19x and 23x (Fig. 1).

Tumor inoculation and measurement. The LLC cell line was obtained from the Cancer Centre, Sun Yet-sen University and cultured in Dulbecco's modified Eagle's medium (DMEM) supplemented with 10% fetal bovine serum (FBS), penicillin (100 U/ml), and streptomycin (100 U/ml). Ten days after the onset of the experimental CJL, LLC cells (0.2 ml, $5x10^6$/ml) were injected subcutaneously into both flanks of mice. Two perpendicular diameters (mm) of each tumor were measured every 4 days with a caliper. Tumor volume (mm^3) was calculated as: tumor volume = (length x $width^2$)/2. The body weights of the mice were monitored during the experiment and no statistically significant difference was found between the LD and CJL groups.

Four mice from the LD group were sacrificed at each time point (ZT3, 7, 11, 15, 19 and 23) and the same number of jet lag mice were sacrificed at the corresponding time points (ZT3x, 7x, 11x, 15x, 19x and 23x; Fig. 1). The lungs, livers and tumors were aseptically removed. The whole lung was fixed with Bouin's fixative. One part of liver and tumor of the host animals were dissected in RNase-free Hank's medium and immediately placed into storage reagent (RNAlater, Ambion, Inc., Austin, TX, USA) on ice, then stored at -80˚C until RNA extraction. Another part of the liver and the tumor tissue were placed into 10% buffered formalin for 24 h. Hematoxylin and eosin (H&E) stained sections were prepared by standard techniques.

cDNA microarray. The differential display of genes from the liver and tumor samples from two mice in each group at two selected time points (ZT7 and 19, LD group; and ZT7x and 19x, CJL group) was detected using a cDNA gene chip (GeneChip® Mouse Genome 430A 2.0 Array, Affymetrix,

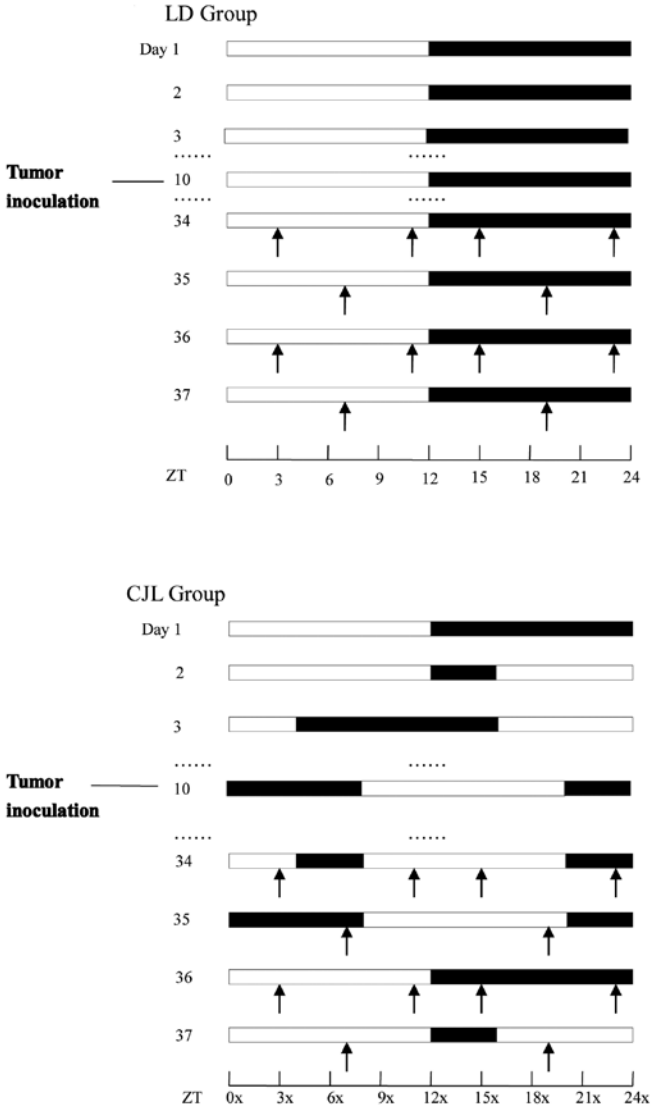

Figure 1. Light regimens: (A) control (LD) group: LD 12:12; (B) chronic jet lag (CJL) group: scheme advancing light onset 8 h for 48 h. Open and black boxes represent light and darkness respectively. Arrows show the sampling time. Day numbers are the experimental chronic jet lag days. The dash points indicate the light schedule. The inoculation of the tumor was performed on Day 10.

Santa Clara, CA, USA), which is a single array representing ~14,000 well-characterized mouse genes.

Total RNA was extracted from the frozen liver and tumor specimens using the RNeasy Mini kit® (Qiagen, Valencia, CA, USA) following the instructions of the manufacturer. The amount of RNA was measured spectrophotometrically by the absorbance at 260 nm. Extracted RNA purity was assessed by the ratio of the absorbance at 260 and 280 nm ($OD_{260/280}$). The RNA was stored at -80˚C after preparation.

The GeneChip® 3' IVT Express kit was used to synthesize first-strand cDNA from total RNA by reverse transcription. This cDNA was then converted into a double-stranded DNA template for transcription. During *in vitro* transcription, amplified RNA was synthesized and a biotin-conjugated nucleotide was incorporated. The amplified RNA was purified, and then hybridized to the chip. After hybridization, the chip was washed, stained using the GeneChip® Hybridization, Wash,

and Stain Kit (Affymetrix), and scanned on a chip reader (Affymetrix).

Microarray data analysis. Robust multichip analysis (RMA) was performed using the Affymetrix Expression Console software (Affymetrix). Principal component analysis (PCA) and hierarchical clustering analysis were performed with the Partek GS 6.4 software (Partek® Genomics Suite™, Partek Inc., St. Louis, MO, USA). The differences in gene expression patterns were designated as significantly different if a >2-fold difference was observed between the two groups.

The molecular functions and pathways of the identified genes were analyzed by Ingenuity Pathway Analysis (IPA; Ingenuity 8.5-2803, Ingenuity System Inc., Redwood City, CA, USA) and the Database for Annotation, Visualization and Integrated Discovery (DAVID) v6.7 (13,14).

Real-time quantitative RT-PCR. The selected genes identified using the cDNA microarray were quantified by real-time quantitative RT-PCR. Two-step real-time quantitative RT-PCR was performed. Reverse transcription was performed at 42˚C for 60 min using the RevertAid First Strand cDNA Sythesis kit (Fermentas, Burlington, ON). Real-time PCR was performed using the Maxima® SYBR-Green qPCR Master Mix (2X) kit (Fermentas). The real-time quantitative PCR conditions were: pre-denaturation at 95˚C for 10 min, denaturation at 95˚C for 15 sec, annealing at 60˚C for 35 sec, and extension for 30 sec (40 cycles) followed by a reaction as 95˚C for 15 sec, 60˚C for 30 sec, 95˚C for 15 sec. Primer sequences were as follows: forward 5'-ATGTGCAGCTGATAAAGACTGG-3' and reverse 5'-AGGCCTTGACCTTTTCAGTAAG-3' (m36B4); forward 5'-GTGAAGCAGGTGAAGGCTAATG-3' and reverse 5'-AAGCTTGTAAGGGGTGGTGTAG-3' (mPer2); forward 5'-AAGAGTTGTGAGGCTGGCAC-3' and reverse 5'-GCTCAAACTTCTGGCCTTTG-3' (PTPRC); forward 5'-AGCGGCAGGTTACATTCAAA-3' and reverse 5'-CAAGTTTTGGTGGCACACAG-3' (CD44); forward 5'-GTGAGGATGACAGGACGGTT-3' and reverse 5'-AAAAGGGGAGAGCATCACTG-3' (NDRG1). The specificity of the PCR products was assessed by the melting curve analysis, and by agarose gel electrophoresis, to check for the presence of non-specific products and to confirm that the size of the product corresponded to that of the expected amplicon. The relative levels of each mRNA of the genes of interest were normalized to the corresponding 36B4 RNA levels by the following formula: relative mRNA level = $2^{-\Delta\Delta Ct}$. The Ct (cycle threshold) is defined as the number of cycles required for the fluorescent signal to cross the threshold (ie, exceeds background level) (15).

Statistical analyses. Statistical tests were performed by SPSS 13.0 software (SPSS Inc., Chicago, IL, USA). Body temperature, body weight, tumor volume, and mRNA relative level of selected genes in the text and figures are mean ± standard error of the mean (SEM). Differences between the groups in above variables across the sampling days were analyzed using a two-way analysis of variance (ANOVA) test.

The differences in the number of palpable tumors, metastases in the liver or lungs were analyzed by the χ^2 test. The periods of temperature and mRNA relative levels of selected target genes in both groups were evaluated by the Reverse Elliptic Spectrum algorithm (6,16,17) using the software for the Research of Biological Rhythms (Cancer Centre, Sun Yat-sen University). Body temperatures and target genes were also analyzed by cosinor analysis (18). A P-value <0.05 was considered to indicate statistically significant differences.

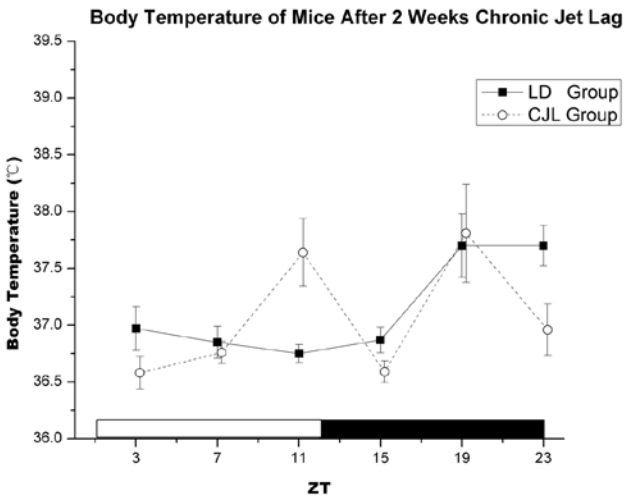

Figure 2. Circadian variation of body temperature in C57BL/6 mice after 10 days experimental chronic jet lag. Each point represents as the mean ± SEM of 5 or 6 mice in the LD group (■) or in the CJL group (○). Open and black boxes represent light and darkness respectively for the LD mice. Body temperature in the CJL group (n=4) were measured at the same time points, labeled as zeitgeber time (ZT) 3x, 7x, 11x, 15x, 19x, and 23x.

Results

Body temperature. Prior to the onset of the experimental CJL, mice in both groups displayed similar circadian rhythms according to the time and the acrophases within the darkness. Ten days after experimental CJL, the mice of the control group continued to have a clear circadian rhythm and the peak time of the body temperature was located at the darkness (period, 24 h, cosinor analysis, P<0.0001). On the other hand, the mice of the CJL group changed to an ultradian rhythm with a period of 10.10 h (cosinor analysis, P<0.0001; Fig. 2). No statistically significant difference of the rhythm-adjusted mean (Mesor) level of the body temperature was found between the 2 groups according to the experimental chronic jet-lag (ANOVA, F=0.093, P=0.760).

Tumor growth. Ten days after tumor inoculation, tumors became palpable in 10 out of 24 mice in the LD group (41.6%), and 21 out of 24 mice in the CJL group (87.5%; χ^2=9.108, P=0.0025). Twenty-two days after tumor inoculation, prior to tissue sampling, the mean tumor volume was 777.45±115.60 mm^3 in the LD group, while 1237.83±163.13 mm^3 in the CJL group of mice. Prior to the animals being sacrificed, the CJL group of mice had larger tumors (two independent-samples t-test, P=0.026). Therefore, the tumors grew faster in the experimental CJL mice than in the LD mice (ANOVA, CJL, P=0.004; Fig. 3).

Carcinoma metastasis. All of the samples, including the lung and tumor tissues, were examined pathologically. Metastatic

Table I. Functional analysis of genes induced or suppressed by experimental chronic jet lag in the murine liver.

GO ID	Gene ontology	Genes
Induced genes		
GO:0006637	Acyl-CoA metabolic process	ACOT1, ACOT4, ACOT3
GO:0006631	Fatty acid metabolic process	CYP4A10, CYP4A31, ACOT1, ACOT4, ACOT3
GO:0043066	Negative regulation of apoptosis	VNN1, BCL6, HSPA1B, ANGPTL4
GO:0043069	Negative regulation of programmed cell death	VNN1, BCL6, HSPA1B, ANGPTL4
GO:0060548	Negative regulation of cell death	VNN1, BCL6, HSPA1B, ANGPTL4
GO:0043086	Negative regulation of catalytic activity	GADD45G, HSPA1B, ANGPTL4
GO:0042981	Regulation of apoptosis	KLF10, VNN1, BCL6, HSPA1B, ANGPTL4
GO:0043067	Regulation of programmed cell death	KLF10, VNN1, BCL6, HSPA1B, ANGPTL4
GO:0010941	Regulation of cell death	KLF10, VNN1, BCL6, HSPA1B, ANGPTL4
GO:0044092	Negative regulation of molecular function	GADD45G, HSPA1B, ANGPTL4
GO:0001676	Long-chain fatty acid metabolic process	ACOT1, ACOT3
GO:0006732	Coenzyme metabolic process	ACOT1, ACOT4, ACOT3
GO:0055114	Oxidation reduction	CYP4A10, HSDL2, CYP2B9, CYP4A31, CYP4A14, CYP2C38
GO:0006094	Gluconeogenesis	G6PC, PCK1
GO:0051346	Negative regulation of hydrolase activity	HSPA1B, ANGPTL4
GO:0045597	Positive regulation of cell differentiation	KLF10, VNN1, DMBT1
GO:0006090	Pyruvate metabolic process	G6PC, PCK1
GO:0019319	Hexose biosynthetic process	G6PC, PCK1
GO:0051186	Cofactor metabolic process	ACOT1, ACOT4, ACOT3
GO:0051336	Regulation of hydrolase activity	BCL6, HSPA1B, ANGPTL4
GO:0046364	Monosaccharide biosynthetic process	G6PC, PCK1
GO:0051094	Positive regulation of developmental process	KLF10, VNN1, DMBT1
GO:0006641	Triglyceride metabolic process	G6PC, PCK1
GO:0046165	Alcohol biosynthetic process	G6PC, PCK1
GO:0006639	Acylglycerol metabolic process	G6PC, PCK1
GO:0006662	Glycerol ether metabolic process	G6PC, PCK1
GO:0006638	Neutral lipid metabolic process	G6PC, PCK1
GO:0045580	Regulation of T cell differentiation	VNN1, BCL6
GO:0018904	Organic ether metabolic process	G6PC, PCK1
Suppressed genes		
GO:0000279	M phase	CCNB1, FMN2, CCNB2, NUF2, CDC20, BIRC5, ANLN, CEP55, CDCA5, CCNA2, HELLS, RAD51
GO:0022403	Cell cycle phase	CCNB1, FMN2, CCNB2, NUF2, CDC20, BIRC5, ANLN, CEP55, CDCA5, CCNA2, HELLS, RAD51
GO:0000280	Nuclear division	CCNB1, CCNB2, NUF2, CDC20, BIRC5, ANLN, CEP55, CDCA5, CCNA2, HELLS
GO:0007067	Mitosis	CCNB1, CCNB2, NUF2, CDC20, BIRC5, ANLN, CEP55, CDCA5, CCNA2, HELLS
GO:0000087	M phase of mitotic cell cycle	CCNB1, CCNB2, NUF2, CDC20, BIRC5, ANLN, CEP55, CDCA5, CCNA2, HELLS
GO:0048285	Organelle fission	CCNB1, CCNB2, NUF2, CDC20, BIRC5, ANLN, CEP55, CDCA5, CCNA2, HELLS
GO:0051301	Cell division	CCNB1, FMN2, CCNB2, NUF2, CDC20, BIRC5, ANLN, CEP55, CDCA5, CCNA2, HELLS
GO:0022402	Cell cycle process	CCNB1, FMN2, CCNB2, NUF2, CDC20, BIRC5, ANLN, CEP55, CDCA5, CCNA2, HELLS, RAD51
GO:0000278	Mitotic cell cycle	CCNB1, CCNB2, NUF2, CDC20, BIRC5, ANLN, CEP55, CDCA5, CCNA2, HELLS
GO:0007049	Cell cycle	CCNB1, FMN2, CCNB2, NUF2, CDC20, BIRC5, ANLN, CEP55, CDCA5, CCNA2, HELLS, RAD51

Table I. Continued.

GO ID	Gene ontology	Genes
GO:0006953	Acute-phase response	SAA2, SAA1, ORM2, FN1
GO:0051303	Establishment of chromosome localization	FMN2, BIRC5, CDCA5
GO:0050000	Chromosome localization	FMN2, BIRC5, CDCA5
GO:0007059	Chromosome segregation	FMN2, NUF2, BIRC5, CDCA5
GO:0002526	Acute inflammatory response	SAA2, SAA1, ORM2, FN1
GO:0000910	Cytokinesis	FMN2, BIRC5, ANLN
GO:0006879	Cellular iron ion homeostasis	HAMP2, HAMP, SCARA5
GO:0006952	Defense response	HAMP2, SAA2, HAMP, SAA1, CLEC2H, ORM2, FN1
GO:0051656	Establishment of organelle localization	FMN2, BIRC5, CDCA5
GO:0055072	Iron ion homeostasis	HAMP2, HAMP, SCARA5
GO:0044270	Nitrogen compound catabolic process	ALDH1L1, NUDT7, UPP2
GO:0046700	Heterocyclic catabolic process	ALDH1L1, NUDT7, MOXD1
GO:0051640	Organelle localization	FMN2, BIRC5, CDCA5
GO:0050832	Defense response to fungus	HAMP2, HAMP
GO:0006631	Fatty acid metabolic process	SCD1, LYPLA2, ACACB, AACS
GO:0007010	Cytoskeleton organization	FMN2, NISCH, NUF2, BIRC5, PSTPIP2
GO:0055114	Oxidation reduction	SCD1, CYP2C55, ALDH1L1, RRM2, HSD3B5, CYP2B10, MOXD1
GO:0007017	Microtubule-based process	FMN2, NUF2, BIRC5, KIF20A
GO:0009132	Nucleoside diphosphate metabolic process	RRM2, NUDT7
GO:0006954	Inflammatory response	SAA2, SAA1, ORM2, FN1
GO:0009620	Response to fungus	HAMP2, HAMP
GO:0000226	Microtubule cytoskeleton organization	FMN2, NUF2, BIRC5
GO:0019058	Viral infectious cycle	D17H6S56E-5, EG665955
GO:0006259	DNA metabolic process	RRM2, SFPQ, HELLS, RAD51, NFIB
GO:0022415	Viral reproductive process	D17H6S56E-5, EG665955
GO:0030005	Cellular di-, tri-valent inorganic cation homeostasis	HAMP2, HAMP, SCARA5

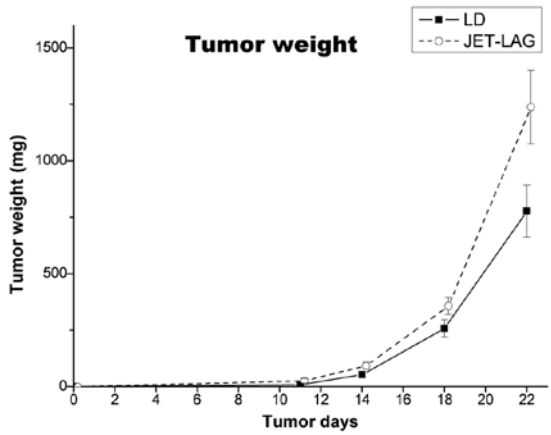

Figure 3. Tumor volume (mean ± SE) after inoculation with Lewis lung carcinoma (LLC) on Day 0. LD, control group; CJL, chronic jet lag group. Effect of the photoperiodic regimen on tumor growth, ANOVA, P=0.004.

tumor was found on the surface of the lung in one mouse of the LD group, and in four mice of the CJL group. The lung H&E-stained sections showed that 10 out of 24 mice had lung metastases in the CJL group, compared to only three mice with lung metastases in the LD group (χ^2=5.17, P=0.023).

cDNA microarray of the tumor and liver. The whole genome cDNA microarrays, which had ~14,000 well-identified genes, were used to detect the effects of the circadian disruption caused by experimental CJL on gene expression in the liver and tumor. The microarray data showed that circadian rhythm had an effect on gene expression, not only for the clock genes, but also for many other genes, such as the genes involved in angiogenesis, the cell cycle, DNA repair, and signal transduction. In the livers of the LD mice, the cDNA microarray data showed that the expression of 189 genes was higher at ZT7 (light) compared to ZT19 (darkness), while the expression of 159 genes was lower. In the tumors of the LD mice, the expression of 130 genes was higher at ZT7 (light) compared to ZT19 (darkness), while the expression of 372 genes was lower.

Gene expression in both the liver and the tumor were also altered by the experimental CJL. Cluster analysis showed that a total of 130 genes were involved in the circadian disrup-

Table II. Functional analysis of genes induced or suppressed by experimental chronic jet lag in Lewis lung tumor.

GO ID	Gene ontology	Genes
Induced genes		
GO:0006955	Immune response	H2-EA, ICAM1, PTPRC, CCR5, SERPINA3G, CCR2, H2-EB1, TLR1, CXCL9, TGTP1, IGH-6, RMCS5
GO:0019882	Antigen processing and presentation	H2-EA, ICAM1, H2-EB1, IGH-6, RMCS5
GO:0002504	Antigen processing and presentation of peptide or polysaccharide antigen via MHC class II	H2-EA, H2-EB1, RMCS5
GO:0006952	Defense response	H2-EA, PTPRC, CCR5, STAB1, CR2, TLR1, CXCL9, COTL1
GO:0009967	Positive regulation of signal transduction	HHEX, PTPRC, DOCK2, ZEB2, IGH-6
GO:0010647	Positive regulation of cell communication	HHEX, PTPRC, DOCK2, ZEB2, IGH-6
GO:0045860	Positive regulation of protein kinase activity	PTPRC, TLR1, ZEB2, IGH-6
GO:0006954	Inflammatory response	CCR5, STAB1, CCR2, TLR1, CXCL9
GO:0002252	Immune effector process	H2-EA, ICAM1, PTPRC, IGH-6
GO:0009611	Response to wounding	CCR5, STAB1, CCR2, TLR1, CXCL9, PAPSS2
GO:0033674	Positive regulation of kinase activity	PTPRC, TLR1, ZEB2, IGH-6
GO:0051347	Positive regulation of transferase activity	PTPRC, TLR1, ZEB2, IGH-6
GO:0019221	Cytokine-mediated signaling pathway	IIGP1B, CCR2, LIFR
GO:0030177	Positive regulation of Wnt receptor signaling pathway	HHEX, ZEB2
GO:0043406	Positive regulation of MAP kinase activity	PTPRC, ZEB2, IGH-6
GO:0043085	Positive regulation of catalytic activity	PTPRC, PTGER4, TLR1, ZEB2, IGH-6
GO:0045059	Positive thymic T cell selection	PTPRC, DOCK2
GO:0032268	Regulation of cellular protein metabolic process	PTPRC, CPEB2, ZEB2, IGH-6,QK
GO:0045060	Negative thymic T cell selection	PTPRC, DOCK2
GO:0043368	Positive T cell selection	PTPRC, DOCK2
GO:0043383	Negative T cell selection	PTPRC, DOCK2
GO:0002449	Lymphocyte mediated immunity	H2-EA, ICAM1, IGH-6
GO:0044093	Positive regulation of molecular function	PTPRC, PTGER4, TLR1, ZEB2, IGH-6
GO:0045859	Regulation of protein kinase activity	PTPRC, TLR1, ZEB2, IGH-6
GO:0002250	Adaptive immune response	H2-EA, ICAM1, IGH-6
GO:0002460	Adaptive immune response based on somatic recombination of immune receptors built from immunoglobulin superfamily domains	H2-EA, ICAM1, IGH-6
GO:0043405	Regulation of MAP kinase activity	PTPRC, ZEB2, IGH-6
GO:0043549	Regulation of kinase activity	PTPRC, TLR1, ZEB2, IGH-6
GO:0021846	Cell proliferation in forebrain	HHEX, ZEB2
GO:0007159	Leukocyte adhesion	ICAM1, PTPRC
GO:0050853	B cell receptor signaling pathway	PTPRC, IGH-6
GO:0002443	Leukocyte mediated immunity	H2-EA, ICAM1, IGH-6
GO:0051338	Regulation of transferase activity	PTPRC, TLR1, ZEB2, IGH-6
GO:0045061	Thymic T cell selection	PTPRC, DOCK2
GO:0043408	Regulation of MAPKKK cascade	PTPRC, ZEB2, IGH-6
GO:0051251	Positive regulation of lymphocyte activation	H2-EA, PTPRC, IGH-6
GO:0019886	Antigen processing and presentation of exogenous peptide antigen via MHC class II	H2-EA, H2-EB1
GO:0002495	Antigen processing and presentation of peptide antigen via MHC class II	H2-EA, H2-EB1
GO:0002696	Positive regulation of leukocyte activation	H2-EA, PTPRC, IGH-6
GO:0050867	Positive regulation of cell activation	H2-EA, PTPRC, IGH-6
GO:0007507	Heart development	MEF2C, PTPRJ, HHEX, CHD7
GO:0042330	Taxis	C3AR1, DOCK2, EAR3
GO:0006935	Chemotaxis	C3AR1, DOCK2, EAR3

Table II. Continued.

GO ID	Gene ontology	Genes
GO:0045058	T cell selection	PTPRC, DOCK2
GO:0007243	Protein kinase cascade	PTPRC, TLR1, MAPK8, IGH-6
GO:0000165	MAPKKK cascade	PTPRC, MAPK8, IGH-6
GO:0007626	Locomotory behavior	C3AR1, DOCK2, EAR3, CHD7
GO:0016525	Negative regulation of angiogenesis	HHEX, STAB1
GO:0030890	Positive regulation of B cell proliferation	PTPRC, IGH-6
GO:0002478	Antigen processing and presentation of exogenous peptide antigen	H2-EA, H2-EB1
GO:0019835	Cytolysis	GZME, FGL2
Suppressed genes		
GO:0030005	Cellular di-, tri-valent inorganic cation homeostasis	ALAS2, HIF1A, MT2, MT1, APLP2
GO:0006873	Cellular ion homeostasis	ALAS2, HIF1A, SNCA, MT2, MT1, APLP2
GO:0055066	Di-, tri-valent inorganic cation homeostasis	ALAS2, HIF1A, MT2, MT1, APLP2
GO:0042592	Homeostatic process	HBA-A1, HSPA1L, ALAS2, HIF1A, SNCA, MT2, MT1, APLP2
GO:0055082	Cellular chemical homeostasis	ALAS2, HIF1A, SNCA, MT2, MT1, APLP2
GO:0030003	Cellular cation homeostasis	ALAS2, HIF1A, MT2, MT1, APLP2
GO:0050801	Ion homeostasis	ALAS2, HIF1A, SNCA, MT2, MT1, APLP2
GO:0055080	Cation homeostasis	ALAS2, HIF1A, MT2, MT1, APLP2
GO:0019725	Cellular homeostasis	ALAS2, HIF1A, SNCA, MT2, MT1, APLP2
GO:0019835	Cytolysis	GZMD, GZMF, GZMG
GO:0048878	Chemical homeostasis	ALAS2, HIF1A, SNCA, MT2, MT1, APLP2
GO:0007626	Locomotory behavior	CCL3, S100A8, SNCA, S100A9, APLP2
GO:0007263	Nitric oxide mediated signal transduction	MT2, MT1
GO:0002246	Healing during inflammatory response	HIF1A, CD44
GO:0010273	Detoxification of copper ion	MT2, MT1
GO:0035239	Tube morphogenesis	HIF1A, ADM, CD44, GJA1
GO:0042541	Hemoglobin biosynthetic process	ALAS2, HIF1A
GO:0007610	Behavior	CCL3, S100A8, SNCA, S100A9, APLP2
GO:0006882	Cellular zinc ion homeostasis	MT2, MT1
GO:0046688	Response to copper ion	MT2, MT1
GO:0055069	Zinc ion homeostasis	MT2, MT1
GO:0030097	Hemopoiesis	HBA-A1, ALAS2, HIF1A, HBB-B1
GO:0020027	Hemoglobin metabolic process	ALAS2, HIF1A
GO:0006091	Generation of precursor metabolites and energy	CYBB, SNCA, PFKP, ERO1L
GO:0035295	Tube development	HIF1A, ADM, CD44, GJA1
GO:0015671	Oxygen transport	HBA-A1, HBB-B1
GO:0001701	*In utero* embryonic development	HBA-A1, HIF1A, ADM, GJA1
GO:0006935	Chemotaxis	CCL3, S100A8, S100A9
GO:0042330	Taxis	CCL3, S100A8, S100A9
GO:0022900	Electron transport chain	CYBB, SNCA, ERO1L
GO:0042060	Wound healing	HIF1A, CD44, GJA1
GO:0048534	Hemopoietic or lymphoid organ development	HBA-A1, ALAS2, HIF1A, HBB-B1
GO:0015669	Gas transport	HBA-A1, HBB-B1
GO:0008219	Cell death	GZMD, PDCD6IP, NIACR1, GZMF, GZMG
GO:0002520	Immune system development	HBA-A1, ALAS2, HIF1A, HBB-B1
GO:0016265	Death	GZMD, PDCD6IP, NIACR1, GZMF, GZMG
GO:0042981	Regulation of apoptosis	HSPA1L, SERINC3, HIF1A, SNCA, NIACR1
GO:0043067	Regulation of programmed cell death	HSPA1L, SERINC3, HIF1A, SNCA, NIACR1
GO:0010941	Regulation of cell death	HSPA1L, SERINC3, HIF1A, SNCA, NIACR1
GO:0009611	Response to wounding	CCL3, HIF1A, CD44, GJA1

Table II. Continued.

GO ID	Gene ontology	Genes
GO:0034599	Cellular response to oxidative stress	HIF1A, SNCA
GO:0001947	Heart looping	HIF1A, GJA1
GO:0009636	Response to toxin	MT2, MT1
GO:0006879	Cellular iron ion homeostasis	ALAS2, HIF1A
GO:0033554	Cellular response to stress	HSPA1L, HIF1A, SNCA, ERO1L
GO:0043009	Chordate embryonic development	HBA-A1, HIF1A, ADM, GJA1
GO:0002274	Myeloid leukocyte activation	SNCA, NDRG1
GO:0055072	Iron ion homeostasis	ALAS2, HIF1A
GO:0009792	Embryonic development ending in birth or egg hatching	HBA-A1, HIF1A, ADM, GJA1
GO:0044057	Regulation of system process	SNCA, GJA1, NIACR1

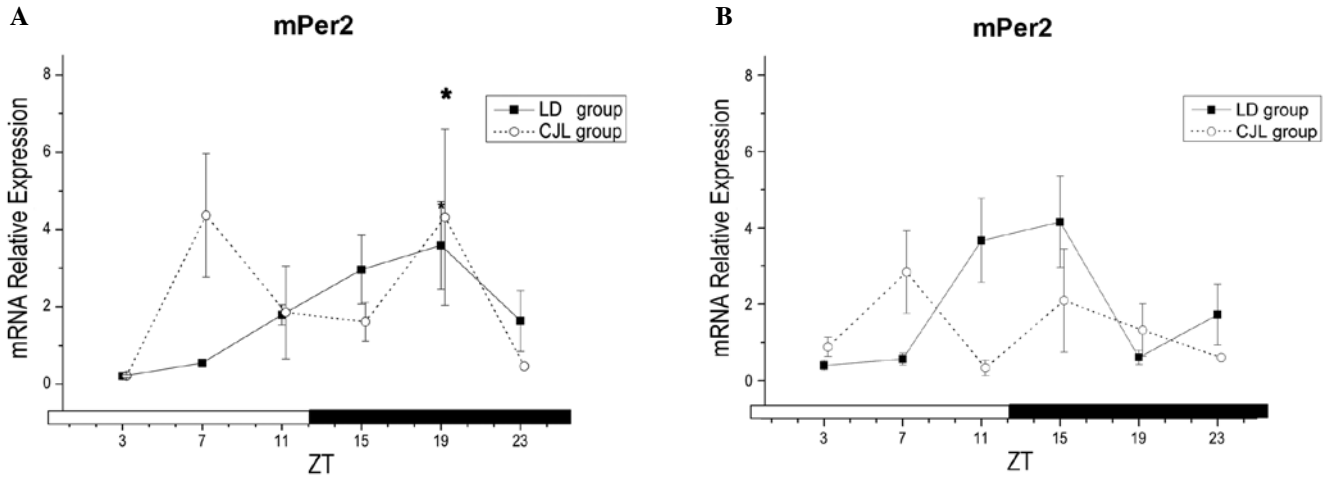

Figure 4. Circadian variation of mPer2 expression in the liver and tumors of mice. (A) Circadian variation of mPer2 expression in liver. (B) Circadian variation of mPer2 expression in tumor. *P<0.05 significantly different from ZT3 as per one-way ANOVA with least significant difference test (LSD) in the LD group mice.

tion in the liver (43 genes induced and 87 genes suppressed), and 142 genes were involved in that of the tumor (100 genes induced and 42 genes suppressed; Tables I and II).

Effects of the experimental chronic jet lag on selected genes expression. The selected gene expression profiles of mPer2, PTPRC, CD44, NDRG1 were detected using the real-time quantitative RT-PCR method.

The effects of experimental CJL on mRNA expression of clock gene mPer2 in the mice livers are shown in Fig. 4A and Table III. The animals showed a clear circadian rhythm in the LD group of mice (cosinor analysis, P=0.0009) and the peak time was located at ZT16:57 (14:34-19:28). In the CJL group of mice, CJL markedly altered the circadian expression patterns of mPer2 (Fig. 4A) from a circadian rhythm to a ultradian rhythm for CJL mice (period, 10.10 h, cosinor analysis, P=0.058). Nevertheless, CJL also clearly altered the 24-h patterns of mPer2 expressions in the tumor tissue. In the tumors of the LD group of mice, the 24-h rhythmic pattern in mPer2 were still observed, and the peak was located at the ZT13:00 (09:20-16:42) (cosinor analysis, P=0.0224) (Fig. 4B). However, CJL ablated the rhythmic changes in mPer2 expression in the tumor (cosinor analysis, P>0.05) (Fig. 4B, Table III).

The selected gene expression profiles of PTPRC, CD44, and NDRG1 in the tumor, which were identified by the microarray, were also detected using the real-time quantitative RT-PCR method. Neither the rhythm nor the effect of the CJL was found in mRNA expression of PTPRC and CD44 (Fig. 5, Table IV). However, the mRNA expression level of NDRG1 in the tumor was suppressed by the experimental CJL even though the result was not statistically significant (P=0.093). The Mesor level of NDRG1 in the LD group of mice was 3.501±3.677 and it was 0.998±0.503 in the CJL group of mice. No circadian rhythm of the NDRG1 expression was found in either group of mice (cosinor analysis, P>0.05) (Fig. 5, Table IV).

Discussion

The correlation between the disruption of circadian rhythm and the development of cancer has been identified in both rodent-model and human research studies. These have suggested that circadian rhythm may be an important control point in tumorigenesis and growth. In this study, experimental CJL, produced by an 8-h shift of the light-dark cycle every 2 days, was used to maximally disturb the circadian rhythm of the experimental group. The body temperature of the mice and the clock gene,

Table III. Cosinor analyses of mPer2 genes expression in liver and tumor of C57BL/6 male mice.

			Cosinor analysis		
Tissue	Mesor ± SEM	Period (h)	Acrophase (95% CI) (h:min)	Amplitude (95% CI)	P-value
Liver					
LD	1.801±0.543	24	16:57 (14:34-19:28)	1.658 (0.719-2.598)	0.0009
CJL	2.207±1.197	10.10	07:45	1.963	0.0582
Tumor					
LD	1.543±0.784	24	13:00 (09:20-16:42)	1.768 (0.260-3.277)	0.0224
CJL	1.502±0.981	10.30	06:27	1.369	0.1383

LD, control 12 h light 12 h dark group; CJL, chronic jet lag group

Table IV. Cosinor analyses of selected genes (PTPRC, CD44 and NDRG1) expression in the tumor of C57BL/6 male mice.

			Cosinor analysis		
Variable	Mesor ± SEM	Period (h)	Acrophase (95% CI) (h:min)	Amplitude (95% CI)	P-value
PTPRC					
LD	1.612±0.463	12	00:28 (03:24-09:59)	0.806 (0.011-1.643)	0.0468
CJL	1.272±0.428	21.7	00:00	0.521	0.2568
CD44					
LD	1.488±0.754	24	13:46	0.197	0.9320
CJL	1.331±0.388	23	01:10	0.439	0.3705
NDRG1					
LD	3.501±3.667	24	10:41	5.920	0.1032
CJL	0.998±0.503	12.80	04:21	0.343	0.6253

LD, control 12 h light 12 h dark group; CJL, chronic jet lag group

mPer2, were used to monitor the effect of the experimental CJL on their circadian rhythms. After 10 days of experimental CJL, the rhythmic profile of the body temperature of the mice was changed from a circadian rhythm to an ultradian rhythm, and the period was shortened from 24 h to 10.10 h. At the mRNA level, CJL also markedly altered the circadian expression patterns of mPer2 in the livers from a circadian rhythm to a suggestive ultradian rhythm. Our results are supported by previous reports which have shown that CJL can disrupt the circadian rhythm, including body temperature, local activity, hematological parameters, and even gene expression and the immune system (6,9).

Circadian disruption also accelerated the growth of the inoculated LLC in our C57BL/6 mice. This result is consistent with previous reports as circadian disruption has shown the same effect on Glasgow osteosarcoma (GOS) or pancreatic adenocarcinoma (PO3) (9,10). The rhythm disorder also increased the rate of cancer metastasis to the lungs, which was 41.67% in mice of the CJL group, but only 12.5% in the LD group ($P<0.05$).

In order to investigate the possible molecular reasons underlying the acceleration of tumor growth and induction of metastases caused by circadian disruption, the whole genome scan method was used to detect the effect of circadian rhythm and rhythm disruption on gene expression within the liver and tumor. In the liver, a total of 348 genes were clock-controlled genes (gene expression at ZT19 compared to ZT7 was increased in 159 genes and decreased in 189). The total number of clock-controlled genes was consistent with the studies of Duffield (19), Panda *et al* (20) (335 genes) and Ueda *et al* (21) (393 genes). In the tumor of the LD group of mice, 372 genes were induced at ZT19 compared to the ZT7, while 130 genes were suppressed; therefore, more genes in the tumor (502 genes in total) were clock-controlled genes.

Experimental CJL also altered the gene expression in both the liver and the tumor. The cluster analysis showed that in the liver a total number of 659 genes were involved in the circadian disruption, and in the tumor, 609 genes. Among the genes involved in the liver, 37 were cell cycle genes as categorized by the gene ontology (GO) biological function, 2 genes (Per2 and Dbp) were circadian exercise genes, and 15 genes were immune system process genes (Fig. 6). Among those involved in the tumor, 4 genes were cell cycle genes, 1 gene (epidermal growth factor receptor, EGFR) was a circadian exercise gene, and 27 genes were immune system process genes (Fig. 7).

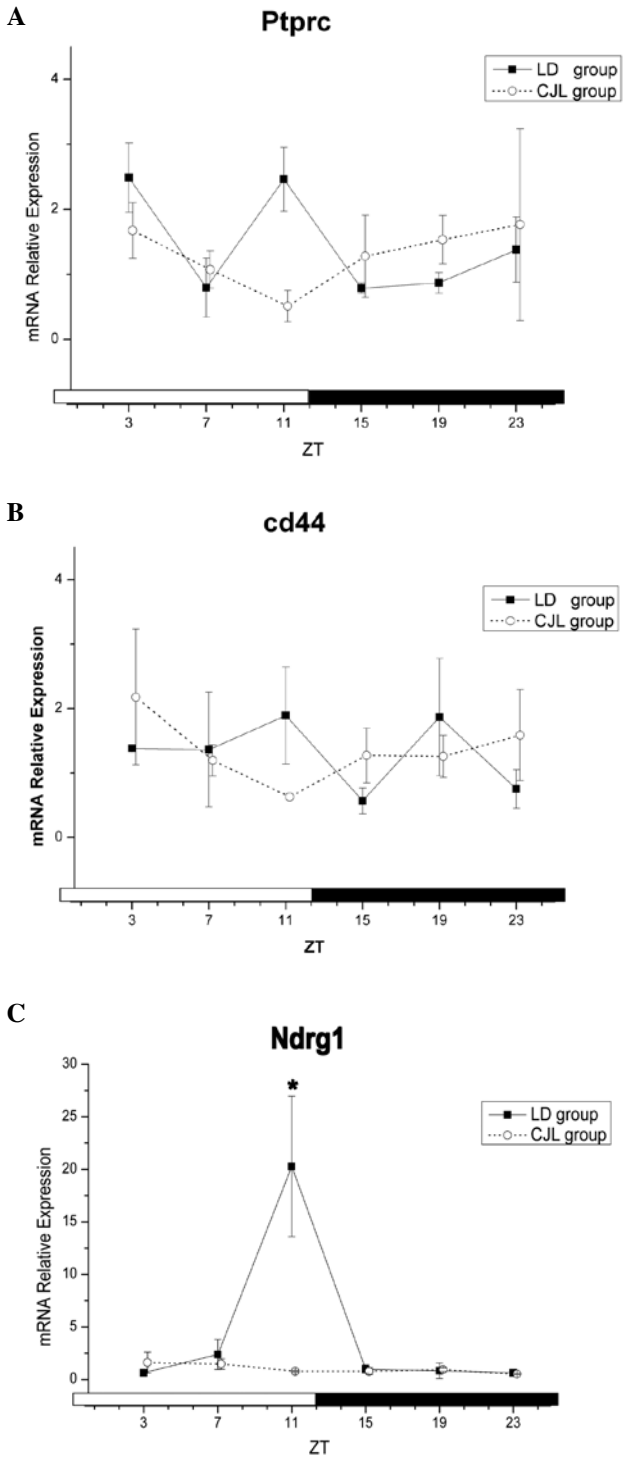

Figure 5. Circadian variation of genes expression in tumors of mice. (A) PTPRC; (B) CD44; (C) NDRG1. *P<0.05 significantly different from ZT3 as per one-way ANOVA with least significant difference test (LSD) in the LD group mice.

In the liver, genes related to the peroxisome proliferator-activated receptors (PPAR) signaling pathway; the cell cycle and the p53 signaling pathway, including CCNA1, CCNB1, CCNB2, and CYP4A were involved. In the tumor, genes related to the following areas were identified, including the cell cycle (GZMD, PDCD6IP, NIACR1, GZMF and GZMG), apoptosis (HSPA1L, SERINC3, HIF1A, SNCA and NIACR1),

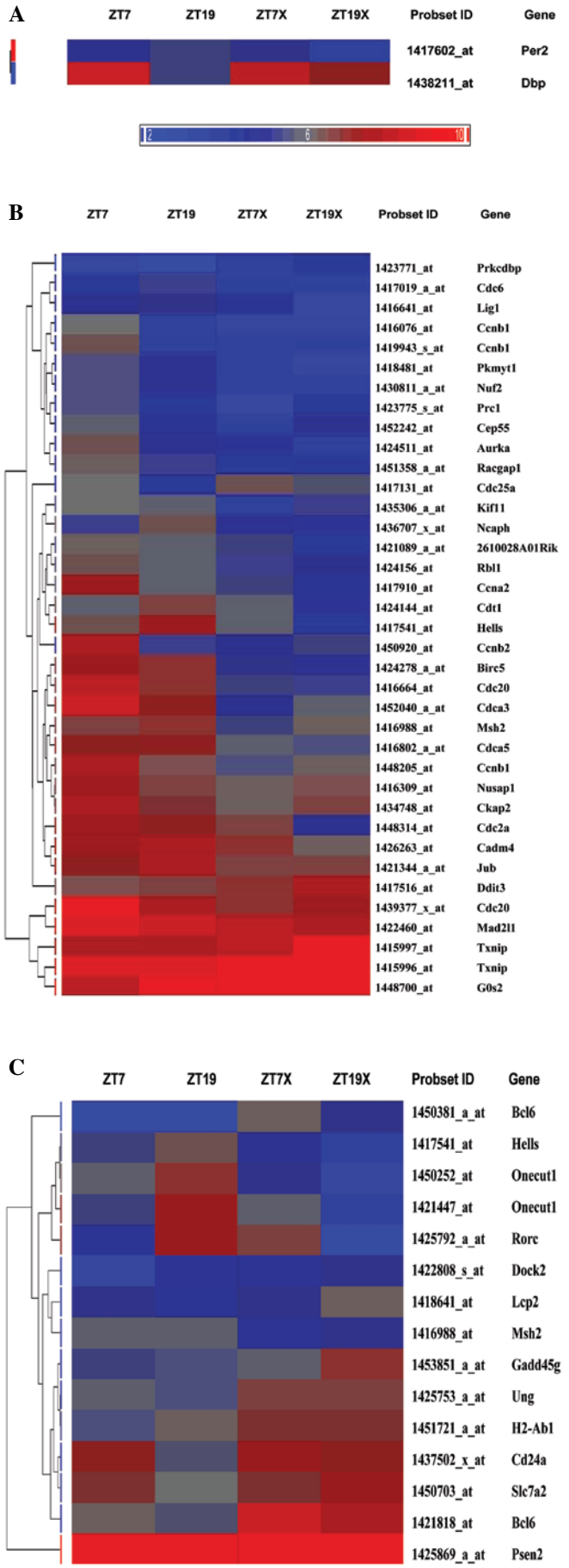

Figure 6. Cluster analysis of gene ontology (GO) biological functions identified genes involved in the circadian disruption in the liver. (A) Cell cycle genes, (B) circadian exercise genes, (C) immune system process genes.

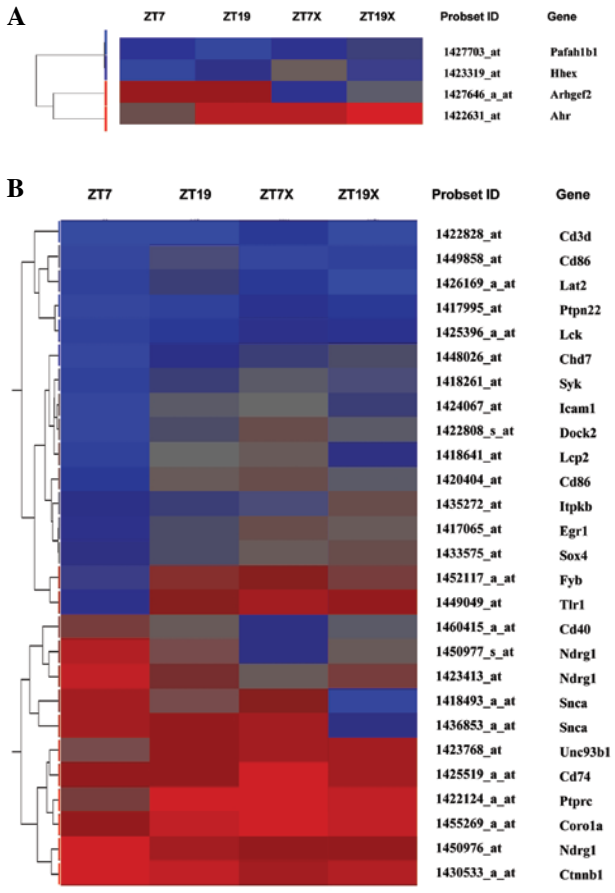

Figure 7. Cluster analysis of gene ontology (GO) biological functions identified genes involved in the circadian disruption in tumors. (A) Cell cycle genes, (B) immune system process genes.

the immune response (H2-EA, ICAM1, PTPRC, CCR5, SERPINA3G, CCR2, H2-EB1, TLR1, CXCL9, TGTP1, IGH-6 and RMCS5), the Wnt signaling pathway (HHEX and ZEB2) and the MAPK signaling pathway (PTPRC, ZEB2, IGH-6 and MAPK8). These genes (shown in Tables I and II) have close relationships with tumor growth, so they may constitute the molecular mechanisms underlying the promotion of tumor growth by disruption of circadian rhythm.

Tumor metastasis is an important clinical problem contributing to the majority of cancer-related deaths. One metastasis suppressor gene, N-myc downstream regulated 1 (NDRG1) was found to be supressed in the CJL mice. The Mesor level of the NDRG1 mRNA expression in the tumor was suppressed by the experimental CJL by about 3-fold. NDRG1 has been shown to be involved in p53-mediated apoptosis and to be regulated by the phosphatase and tensin homolog (PTEN) gene. Its expression was shown to be negatively correlated with tumor metastasis. Studies *in vitro* and *in vivo* have demonstrated a significant reduction in the metastatic ability of cells that overexpression NDRG1 (22). This gene also affects cell cycle, apoptosis, and tumorigenesis through interactions with other proteins; the network of NDRG1 in the tumor is shown in Fig. 8. In this study, the expression of the metastasis suppressor gene, NDRG1, in the tumor was decreased by CJL. This may be one potential explanation for the induction of metastasis by circadian disruption.

In conclusion, jet lag has been shown to change the rhythmic profiles of body temperature, and to have an effect on tumor growth and metastasis. This may be due to the effect of circadian disruption on gene expression, not only of clock genes, but also of tumor-related genes, such as those involved in

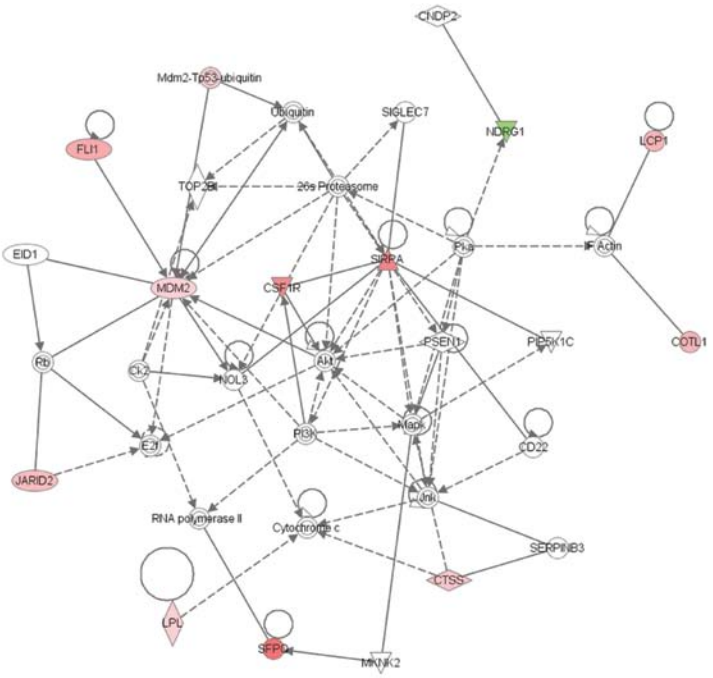

Figure 8. Network of N-myc downstream regulated 1 (NDRG1) constructed by the Ingenuity pathway analysis (IPA). Genes, proteins, and chemicals are displayed as various shapes. The shapes are indicative of the molecular class (protein family, or chemical). Coloring is based on the expression values in the CJL mice compared to the LD mice. Red indicates upregulation (positive values), green downregulation (negative values), gray that the molecule was part of the dataset but did not meet the user-specified cut-off value, and white that the molecule was added from the Ingenuity Knowledge Base. Lines connecting molecules indicate molecular relationships. Dashed lines indicate indirect interactions; solid lines indicate direct interactions. The style of the arrows indicates specific molecular relationships and the directionality of the interaction.

the cell cycle, immunity, and cancer metastasis. It is suggested that circadian disruption can promote tumor progression and metastasis by affecting the expression of both tumor-related and metastasis suppressor genes.

Acknowledgements

We thank Yueli Sun, Bing Yang and Yanru Feng (Sun Yat-sen University) for assistance with the animal experiments; Mr. Yongju Liang (Sun Yat-sen University) for assistance with the cell culture; Mr. Shengzhao Yang (Sun Yat-sen University) for assistance with the software program of the Research of Biological Rhythms, and Dr Gregory Ford (Morehouse School of Medicine, USA) for help with microarray data analysis. We especially thank Dr Jennifer Evans (Morehouse School of Medicine, USA) for helpful discussions and writing modification. We also thank Dr X.M. Li and Dr F. Lévi (INSERM U776, France) for helpful discussions. This study was supported by the National Natural Science Foundation of China (no. 30500589, to M.W.), and by the Scientific Research Foundation for the Returned Overseas Chinese Scholars, State Education Ministry, P.R. China (2005, to M.W.).

References

1. Schibler U and Sassone-Corsi P: A web of circadian pacemakers. Cell 111: 919-922, 2002.
2. Van GR: How the clock sees the light. Nat Neurosci 11: 628-630, 2008.
3. Wu MW, Li XM, Xian LJ and Levi F: Effects of meal timing on tumor progression in mice. Life Sci 75: 1181-1193, 2004.
4. Wu MW, Xian LJ, Li XM, Pasquale I and Francis L: Circadian expression of dihydropyrimidine dehydrogenase, thymidylate synthase, c-myc and p53 mRNA in mouse liver tissue. Ai Zheng 23: 235-242, 2004.
5. Wu MW, Zeng ZL, Li S, *et al*: Circadian variation of plasma cortisol and whole blood reduced glutathione levels in nasopharyngeal carcinoma patients. Ai Zheng 27: 237-242, 2008.
6. Wu M, Cai Y, Sun J, *et al*: Effects of experimental chronic jet lag on hematological and immune parameters in mice. Biol Rhythm Res 41: 363-378, 2010.
7. Fu L and Lee CC: The circadian clock: pacemaker and tumour suppressor. Nat Rev Cancer 3: 350-361, 2003.
8. Fu L, Pelicano H, Liu J, Huang P and Lee C: The circadian gene Period2 plays an important role in tumor suppression and DNA damage response in vivo. Cell 111: 41-50, 2002.
9. Filipski E, Innominato PF, Wu M, *et al*: Effects of light and food schedules on liver and tumor molecular clocks in mice. J Natl Cancer Inst 97: 507-517, 2005.
10. Filipski E, King VM, Li X, *et al*: Host circadian clock as a control point in tumor progression. J Natl Cancer Inst 94: 690-697, 2002.
11. Wood PA, Yang X, Taber A, *et al*: Period 2 mutation accelerates ApcMin/+ tumorigenesis. Mol Cancer Res 6: 1786-1793, 2008.
12. Gery S, Komatsu N, Baldjyan L, Yu A, Koo D and Koeffler HP: The circadian gene per1 plays an important role in cell growth and DNA damage control in human cancer cells. Mol Cell 22: 375-382, 2006.
13. Huang da W, Sherman BT and Lempicki RA: Systematic and integrative analysis of large gene lists using DAVID bioinformatics resources. Nat Protoc 4: 44-57, 2009.
14. Dennis G Jr, Sherman BT, Hosack DA, *et al*: DAVID: database for annotation, visualization, and integrated discovery. Genome Biol 4: P3, 2003.
15. Livak KJ and Schmittgen TD: Analysis of relative gene expression data using real-time quantitative PCR and the 2(-Delta Delta C(T)) Method. Methods 25: 402-408, 2001.
16. Mauvieux B, Gouthiere L, Sesboue B and Davenne D: A study comparing circadian rhythm and sleep quality of athletes and sedentary subjects engaged in night work. Can J Appl Physiol 28: 831-887, 2003 (In French).
17. Mauvieux B, Gouthiere L, Sesboue B, Denise P and Davenne D: Effects of the physical exercise and sports on the circadian rhythm of temperature and waking/sleep pattern of the elderly person. Examples in retired and night workers. Pathol Biol (Paris) 55: 205-207, 2007 (In French).
18. Nelson W, Tong YL, Lee JK and Halberg F: Methods for cosinorrhythmometry. Chronobiologia 6: 305-323, 1979.
19. Duffield GE: DNA microarray analyses of circadian timing: the genomic basis of biological time. J Neuroendocrinol 15: 991-1002, 2003.
20. Panda S, Antoch MP, Miller BH, *et al*: Coordinated transcription of key pathways in the mouse by the circadian clock. Cell 109: 307-320, 2002.
21. Ueda HR, Chen W, Adachi A, *et al*: A transcription factor response element for gene expression during circadian night. Nature 418: 534-539, 2002.
22. Ando T, Ishiguro H, Kimura M, *et al*: Decreased expression of NDRG1 is correlated with tumor progression and poor prognosis in patients with esophageal squamous cell carcinoma. Dis Esophagus 19: 454-458, 2006.